doi.org/10.36721/PJPS.2026.39.8.221.1

p40-engineered CAR T-cells targeting CD276 enhance anti-tumor efficacy in non-small cell lung cancer

Jianye Yang[2] and Ying Chen[1*]
[1]Outpatient Department, Affiliated Hospital of Shaoxing University, Shaoxing, China.
[2]Department of Respiratory and Critical Care Medicine, Affiliated Hospital of Shaoxing University, Shaoxing, China.

Abstract: **Background**: Chimeric antigen receptor (CAR) T-cells have shown remarkable therapeutic efficacy in hematological malignancies; however, effective breakthroughs in solid tumors have not yet been achieved. **Objectives**: This study aimed to explore the therapeutic potential of p40-engineered CAR T-cells targeting CD276 (p40-H3BBz) for the treatment of non-small cell lung cancer (NSCLC). **Methods**: A CAR targeting CD276 (H3BBz) was engineered to co-express the p40 subunit via lentiviral transduction. The function of p40-H3BBz was evaluated by measuring cytokine secretion levels and performing luciferase-based cytotoxicity assays in vitro. In vivo efficacy was assessed using tumor-bearing mouse models, and T-cell infiltration was analyzed by immunohistochemistry. **Results**: The transduction efficiencies of H3BBz and p40-H3BBz were 63.7% and 52.3%, respectively, with both populations predominantly composed of $CD4^+$ T-cells. Upon activation, p40-H3BBz exhibited increased IL-23 secretion, while IL-12 levels were comparable to those of H3BBz in vitro. p40-H3BBz also demonstrated enhanced cytotoxicity, degranulation, and increased production of IL-23 and IFN-γ. In vivo, p40-H3BBz CAR T-cells showed superior tumor growth inhibition, increased T-cell infiltration, and elevated IL-23 levels within tumors, without inducing significant toxicity in major organs. **Conclusion**: p40-H3BBz exhibits enhanced cytokine release and cytotoxic activity, representing a promising and safe therapeutic strategy for the treatment of NSCLC.

Keywords: Chimeric antigen receptor; CD276 antigen; Interleukin 23; Non-small cell lung cancer

Submitted on 24-02-2025 – Revised on 12-11-2025 – Accepted on 13-11-2025

INTRODUCTION

NSCLC is a major high-incidence and fatal tumor type worldwide and there is an urgent need for effective treatment methods (Wang *et al.*, 2021; Qin *et al.*, 2024). While the effect of CAR T-cells in hematological cancers is encouraging (Parikh and Lonial, 2023; Yang *et al.*, 2023), their activity against solid tumors, including NSCLC, has been limited (Hong *et al.*, 2020). This is primarily due to the CAR T-cells' poor infiltration (Allen *et al.*, 2022), persistence (Chan *et al.*, 2024) and activity (Tang *et al.*, 2023) when treating solid tumors.

To address these challenges, this study focused on CD276 (B7-H3), an excellent target antigen for CAR T-cells (Li *et al.*, 2023). CD276 belongs to the B7 molecular family and is highly expressed in many solid tumors, including NSCLC (Altan *et al.*, 2017). Importantly, CD276 expression is minimal in normal tissues (Getu *et al.*, 2023), making it an attractive antigen for CAR T-cell therapy due to its high specificity and low off-target toxicity. Previous studies have demonstrated the feasibility and efficacy of targeting CD276 in various cancer models, further underscoring its relevance as a therapeutic target (Seaman *et al.*, 2017; Yang *et al.*, 2020).

In addition to selecting an appropriate target antigen, enhancing CAR T-cell activity within the tumor microenvironment (TME) is pivotal for improving therapeutic outcomes (Feng *et al.,* 2024). Interleukin-23 (IL-23) consists of p19 and p40 subunits and is crucial for the expansion and survival of memory T-cells (Pawlak *et al., 2022;* Boniface *et al.*, 2008). IL-23 is important for the anti-tumor course of T-cells by promoting the expansion and effector function of cytotoxic T lymphocytes (Ma *et al.*, 2020). Moreover, IL-23 has been shown to support the differentiation and maintenance of Th17 cells, which are known to contribute to anti-tumor responses by secreting pro-inflammatory cytokines and recruiting other immune cells to the TME (Subhadarshani*, et al.*, 2021). Notably, T-cells upregulate the p19 subunit, not the p40 subunit, however, upon activation (Ma *et al.*, 2020). This unique expression pattern offers an opportunity to engineer T-cells to express the p40 subunit, thereby enabling autocrine IL-23 signaling upon T-cell activation.

This study constructed a CAR targeting CD276 and co-expressed the p40 subunit to reinforce its therapeutic effect in NSCLC. It was hypothesized that p40-H3BBz would exhibit superior cytotoxic activity within the TME, thereby improving therapeutic efficacy. Through a series of experiments, it was verified that p40-H3BBz shows better tumor-killing activity, increased cytokine secretion and superior tumor infiltration compared with H3BBz. Moreover, it was shown that p40-H3BBz does not cause significant toxicity, highlighting its potential as a safe and effective treatment for NSCLC.

MATERIALS AND METHODS

Cell source

Cell lines were obtained from the American Type Culture Collection (ATCC). These cell lines were grown in DMEM

**Corresponding author:* e-mail: chen523351795@163.com

(Vivacell) and added 10% FBS (Vivacell). The cells were placed statically in an incubator Forma™ 311 (Thermo Fisher, MA, USA) at 37°C with 5% CO2.

UALCAN analysis of CD276 expression situation and survival state

The mRNA expression levels of CD276 were explored using the UALCAN website (Chandrashekar *et al.*, 2022), which provides an interactive platform for exploring tumor transcriptome data from The Cancer Genome Atlas (TCGA). The prognosis status of CD276 was also evaluated using the survival analysis tools available on the UALCAN website.

Construction of CAR T-cells

The second-generation CAR targeting CD276 was constructed using a lentiviral vector. The CAR construct included a CD8α signal peptide, an anti-CD276 single-chain variable fragment (scFv) (Loo *et al.*, 2012), a CD8α hinge and transmembrane domain and the signaling parts of 4-1BB and CD3ζ. The p40 subunit of IL-23 was co-expressed with the CAR using an internal ribosome entry site (IRES).

Primary human T-cells were isolated from peripheral blood using the manufacturer's isolation kit protocol (Miltenyi Biotec, Germany) and activated with Dynabeads (Thermo Fisher Scientific, CA, USA) for 48 hours. After cells were activated, CD276 CAR or p40-CD276 CAR encoded lentiviruses were added. Transduced T-cells were expanded in RPMI-1640 medium supplemented with 10% FBS, 2 mM GlutaMAX, 100 units/mL penicillin, 100 µg/mL streptomycin and 10 ng/mL IL-2 (PeproTech, CA, USA).

Flow cytometry analysis

Flow cytometry was used to assess CD276 protein expression levels in tumor cell lines and the CAR-positive rate in T-cells. Antibodies against CD276, CD3, CD4 and CD8 (BioLegend, CA, USA) were added to cells for 30 minutes in a dark environment of 4 degrees. For CD107a, cells were incubated with Brefeldin A (Yeasen, Shanghai, China) after 16 hours of co-culture and stained with the CD107a antibody. Data was collected using LSRFortess X-20 (BD Biosciences, CA, USA). All data collected in this work were processed using FlowJo™ v10 software.

Luciferase-based cytotoxicity assay

Luciferase (FFluc) transduced target tumor cells were co-incubated with H3BBz or p40-H3BBz of different effector-to-target (E:T) ratios (3:1, 1:1, 1:3). After co-incubation for 24 hours, the remaining viable target T-cells were counted by measuring luciferase activity. The signal is measured by the microplate reader Synergy HTX (BioTek, VT, USA). Specific cytotoxicity (%) was calculated as follows: Specific cytotoxicity (%) = (1-Spontaneous RLU/Experimental RLU)×100.

Animal experiments

All ethical norms for animal experiments were approved by Shaoxing University. For the *in-vivo* anti-tumor efficacy studies, mice were subcutaneously injected with 5E6 A549 cells in 100 µl pre-cooled PBS. Once tumors reached approximately 100 mm^3, mice were randomly assigned to treatment groups and received an intravenous injection of 1×10^7 Blank T-cells, 1×10^7 H3BBz, or p40-H3BBz. Tumor growth was monitored weekly. Mice were euthanized at the end of the study and tumors and major organs were collected for further analysis. The tumor volume is calculated as Length × Width^2 / 2.

ELISA assays

IL-23, IL-12 and IFN-γ levels were quantified using ELISA kits (Lianke Biotechnology Co., Ltd., Hangzhou, China). Supernatants were collected and analyzed using the respective ELISA kits after incubation with CD3/CD28 Dynabeads or tumor cells for 24 hours. The data was collected with a microplate reader Synergy HTX (BioTek).

Immunohistochemistry analysis

Fresh tissues were fixed in 10% formalin, and 5-µm-thick tissue sections underwent standard pre-treatment and antigen retrieval. Adding antibodies against-CD3 and IL-23 (Proteintech, Wuhan, China), followed by the addition of horseradish peroxidase (HRP)-conjugated secondary antibodies. To detect the target signal, DAB (3,3'-diaminobenzidine) was applied as the chromogenic reagent. Following this, hematoxylin was used to stain cell nuclei. The stained slides were then examined and recorded using a microscope CKX53 (Olympus, Tokyo, Japan).

Hematoxylin and eosin (H&E) staining

Tissue samples, including liver, lung, kidney, heart and spleen, were obtained from mice after euthanasia. Fix the fresh tissue with 10% formalin. Thin sections (5 µm) were prepared and stained using hematoxylin and eosin. Slides were examined microscopically using Olympus equipment CKX53 to assess morphology and identify signs of organ toxicity.

Statistical analysis

All analyses were carried out using GraphPad Prism (v8.0). Data are reported as mean values with corresponding standard deviations. Group differences were examined by either Student's t-test or one-way ANOVA with Tukey's post hoc correction. The *p-value* less than 0.05 was considered statistically significant

RESULTS

CD276 is highly expressed in lung cancer

To determine CD276 expression, the TCGA database was initially queried. A pan-cancer investigation demonstrated marked upregulation of CD276 in most tumors compared with their corresponding adjacent normal tissues (Fig. 1A).

Focusing on NSCLC, it was found that CD276 expression levels in tumor tissues were markedly higher than in normal tissues (Fig. 1B). Furthermore, survival analysis indicated that NSCLC patients with high CD276 expression had significantly poorer survival outcomes, suggesting that CD276 acts as an oncogenic factor (Fig. 1C). To validate these findings, CD276 expression was examined in cell lines and found that normal lung epithelial cells (BEAS-2B) exhibited low CD276 expression, whereas NSCLC cell lines A549 and H1299 showed high CD276 expression (Fig. 1D). These data collectively underscore the therapeutic promise of CD276 in NSCLC, given its elevated expression in tumor tissues.

Production and characterization of p40-H3BBz

In this study, a second-generation CAR targeting CD276 using the 8H9-derived humanized scFv (Loo *et al.*, 2012) and co-expressing the p40 subunit was constructed. The schematic representation of the H3BBz and the p40-H3BBz construct is shown in fig. 2A. Lentiviral transduction was performed to introduce these constructs into CD3+ T-cells (Fig. 2B). The results indicated that the transduction efficiency for H3BBz was 63.7%, while for p40-H3BBz, it was 52.3% (Fig. 2C). To evaluate the CD4 and CD8 subpopulations, the transduced T-cells were analyzed and the proportions of $CD4^+$ and $CD8^+$ T-cells did not differ significantly between the two cohorts. Both engineered T-cell populations were predominantly CD4+ T-cells (Fig. 2D). Furthermore, the engineered T-cells were stimulated and the secretion of IL-23 and IL-12 was measured using ELISA. The results demonstrated that the IL-23 level in the supernatant of p40-H3BBz was higher than that of H3BBz. In contrast, IL-12 levels remained unchanged between the two groups (Fig. 2E). These findings confirm the successful construction and functional validation of p40-H3BBz, which exhibits enhanced IL-23 secretion upon activation.

Enhanced in-vitro cytotoxicity of p40-H3BBz

To evaluate the cytotoxicity of p40-H3BBz, it was co-cultured with luciferase-expressing tumor cell lines (Fig. 3A). The cytotoxicity assays revealed that both H3BBz and p40-H3BBz exhibited significant cytotoxic activity against antigen-high tumor cells, whereas showing minimal cytotoxicity against antigen-low BEAS-2B cells. Notably, p40-H3BBz exhibited greater cytotoxicity than H3BBz (Fig. 3B). Flow cytometry analysis of CD107a expression, a marker of degranulation, further corroborated these findings. p40-H3BBz exhibited enhanced degranulation when incubated with target T-cells compared to H3BBz (Fig. 3C). Additionally, ELISA assays were used to measure cytokines. The results showed that p40-H3BBz produced much more IL-23 and IFN-γ than H3BBz (Fig. 3D). These findings collectively indicate that p40-H3BBz possesses superior *in-vitro* cytotoxic activity and enhanced cytokine secretion, highlighting its potential for effective anti-tumor responses in NSCLC.

Superior in-vivo activity of p40-H3BBz

To test the efficacy of p40-H3BBz *in-vivo*, tumor-bearing mice were infused with either H3BBz or p40-H3BBz. Tumor volume measurements revealed that both H3BBz and p40-H3BBz exhibited tumor-suppressive activity. However, p40-H3BBz demonstrated significantly stronger tumor inhibition compared to H3BBz (Fig. 4A). This enhanced anti-tumor effect was further corroborated by the final tumor weight measurements (Figs. 4B-C). Immunohistochemical analysis of excised tumor tissues showed increased tumor infiltration in the p40-H3BBz group compared with H3BBz-treated groups. Moreover, sections from the p40-engineered group showed significantly higher levels of IL-23 (Figs. 4D-E). To assess the safety profile, H&E staining was performed on key organs collected from treated animals. No evident histopathological abnormalities were detected, indicating that p40-H3BBz did not induce notable toxic side effects (Fig. 4F). These results collectively demonstrate that p40-H3BBz has a better anti-tumor function *n-vivo*, enhanced tumor infiltration and increased IL-23 production within the tumor microenvironment, without causing significant toxicity. This highlights the safety and efficacy of p40-H3BBz when treating NSCLC.

DISCUSSION

In this study, CAR T-cells were designed and generated to target CD276 and co-express the p40 subunit of IL-23 to augment their therapeutic capacity in NSCLC. The findings of this study demonstrate that p40-H3BBz exhibits superior cytotoxicity against CD276-positive tumor cells and greater therapeutic potency than H3BBz in mice. These findings revealed the therapeutic promise of leveraging autocrine IL-23 signaling to improve CAR T-cell efficacy in the immunosuppressive TME of solid tumors.

CD276 is extensively expressed in both tumor cells and their associated vasculature but is hardly expressed in nonmalignant tissues (Seaman *et al.*, 2017). Its overexpression in various malignancies, including prostate cancer (Fan *et al.*, 2023), clear cell renal cancer (Zhang *et al.*, 2024), lung cancer (Zhang *et al.*, 2023) and ovarian cancer (Cai *et al.*, 2020), correlates with reduced tumor-infiltrating lymphocytes, lower cancer severity and poorer prognosis. The distinct expression pattern of CD276 in malignant tissues and nonmalignant tissues highlights its opportunity as an attractive antigen for cancer immunotherapy. The experiments of this study proved that H3BBz could effectively target and eliminate CD276-expressing tumor cells, thereby validating CD276 as a viable therapeutic target. Previous research on CD276 CAR T-cells has demonstrated notable antitumor activity in animal studies (Zhang *et al.*, 2023) and some clinical studies (Hu *et al.*, 2022).

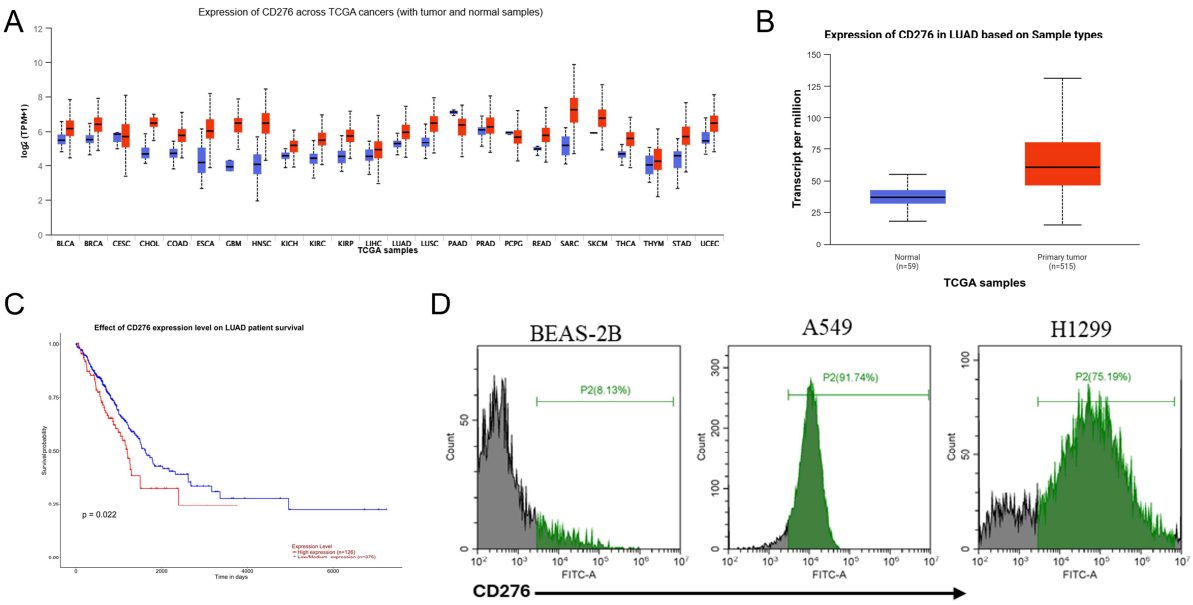

Fig. 1: Expression of CD276 in lung adenocarcinoma (LUAD). (A) Expression levels of CD276 across different tumors in the TCGA database; (B) Expression of CD276 in LUAD tumor tissues compared to adjacent normal tissues in the TCGA database; (C) Kaplan-Meier survival curve illustrating the relationship between CD276 expression and survival in LUAD patients; (D) Flow cytometry analysis of CD276 expression in normal lung epithelial cells and NSCLC cell lines.

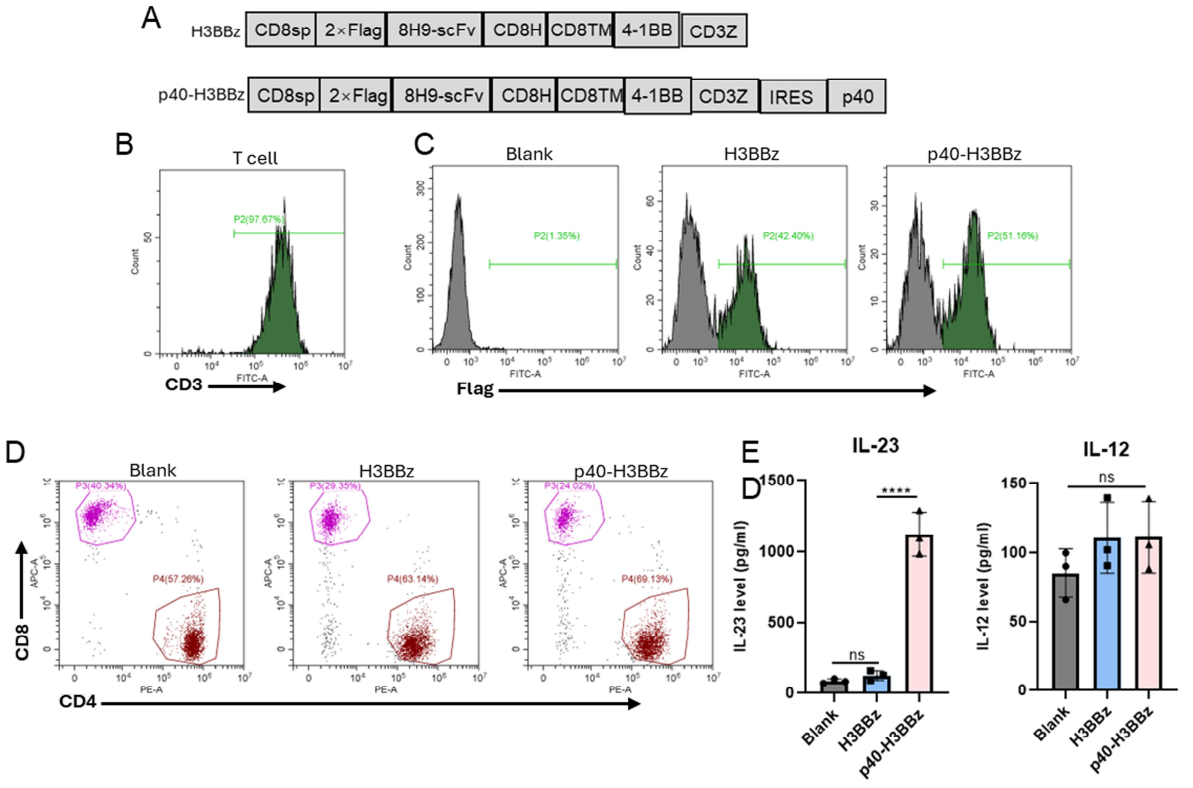

Fig. 2: Construction and validation of CAR-engineered T-cells. (A) Schematic representation of the H3BBz and p40-H3BBz constructs; (B) Flow cytometry results showing the purity of isolated CD3+ T-cells; (C) Flow cytometry analysis of Flag expression in engineered T-cells; (D) Flow cytometry analysis of CD4 and CD8 subpopulations in engineered T-cells. (E) ELISA results showing the expression levels of IL-23 and IL-12 in the supernatant after 24 hours of CD3/CD28 bead activation. ns, $p>0.05$, ****, $p<0.0001$.

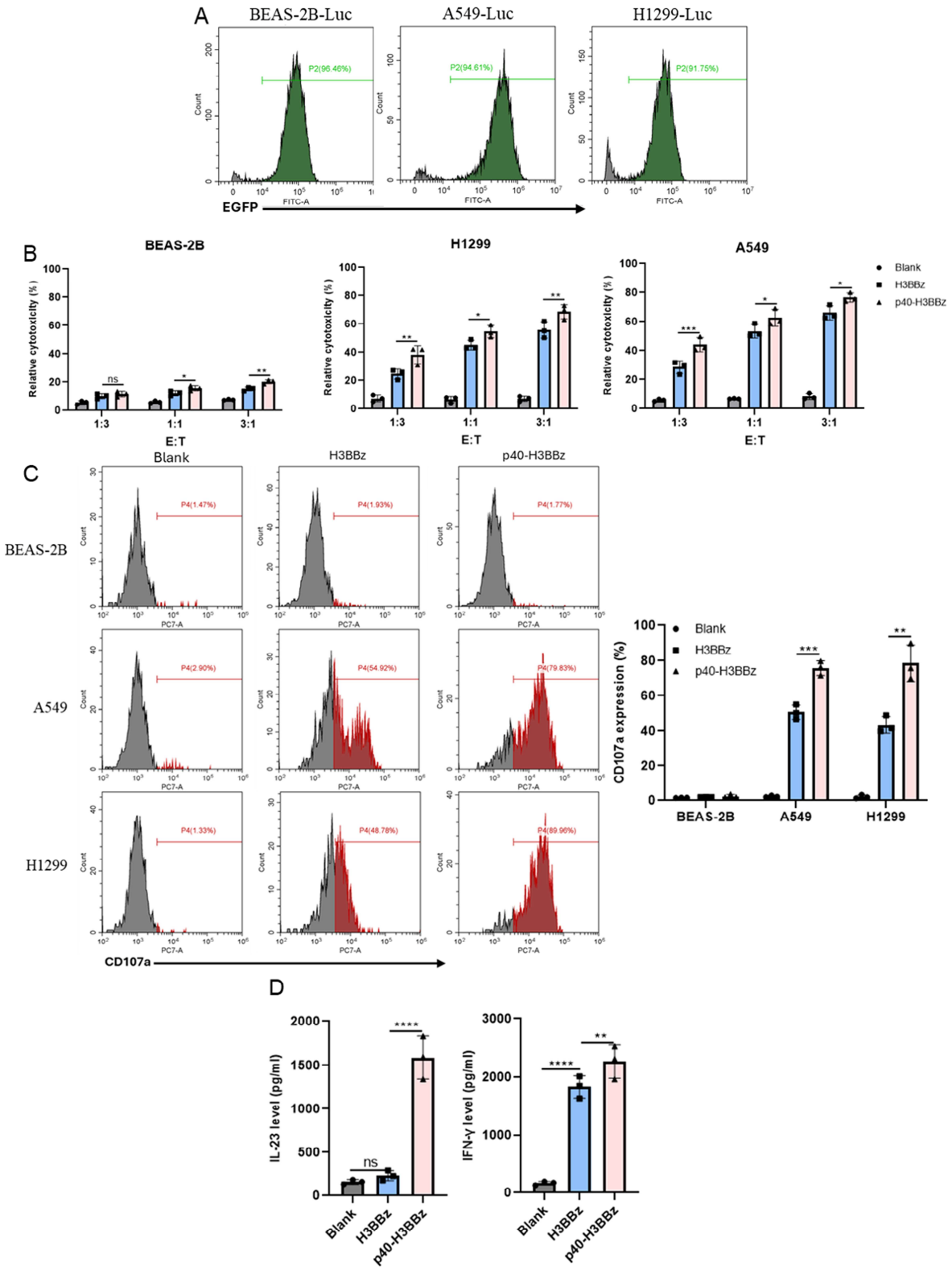

Fig. 3: *In-vitro* activity of CAR-engineered T-cells. (A) Flow cytometry analysis of the transfection efficiency of luciferase-expressing cells; (B) Cytotoxicity assay based on luciferase activity after 24 hours of co-culture at various E:T ratios; (C) Flow cytometry analysis of CD107a expression in T-cells after 16 hours of co-culture at a 3:1 E:T ratio; (D) ELISA results showing the levels of IL-23 and IFN-γ in the supernatant after 24 hours of co-culture at a 3:1 E:T ratio. ns, $p>0.05$, *, $p<0.05$, **, $p<0.01$, ***, $p<0.001$, ****, $p<0.0001$.

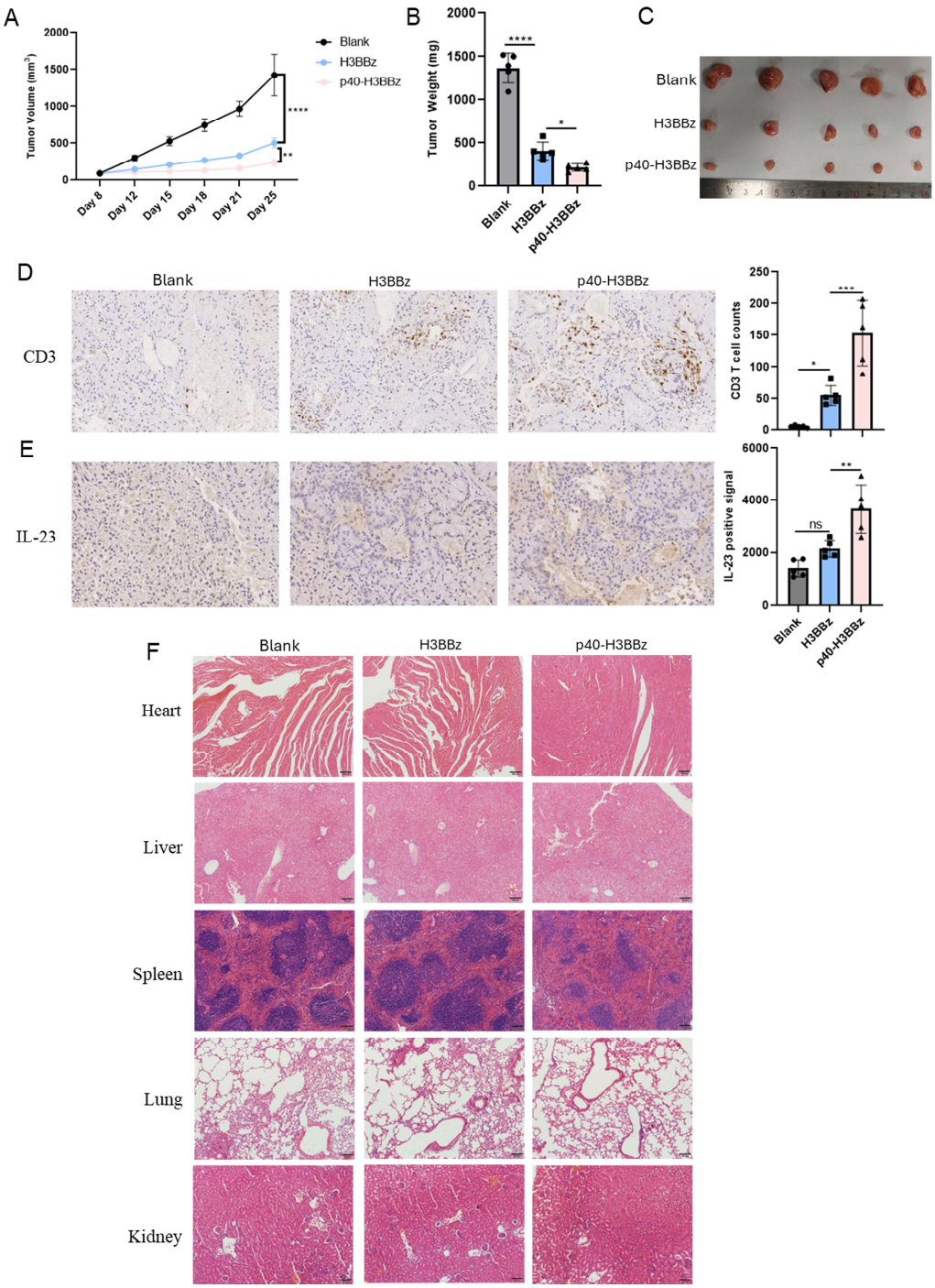

Fig. 4: *In-vivo* anti-tumor efficacy of CAR-engineered T-cells. (A) Tumor volume monitoring results after T-cell infusion on day 8; (B) Tumor weight results after euthanizing the mice; (C) Photographs of tumors from euthanized mice; (D) IHC analysis of CD3+ T-cell infiltration in tumors; (E) IHC analysis of IL-23 levels in tumors; (F) H&E staining results of major organs to assess potential toxicity. ns, $p>0.05$, *, $p<0.05$, **, $p<0.01$, ***, $p<0.001$, ****, $p<0.0001$.

However, the overall therapeutic efficacy remains suboptimal. In a clinical study targeting glioblastoma, the administration of up to 1×10^9 CD276 CAR T-cells via intraventricular injection yielded limited clinical benefits (Vitanza *et al.*, 2023). Several methods were developed to enhance CAR T-cell activity by engineering them to secrete various cytokines. For instance, IL-15 and IL-18 have been co-expressed with CARs to improve their proliferation, survival and effector function. While these approaches have shown promise, they are not without drawbacks. IL-15 can lead to the expansion of regulatory T-cells (Tregs), which could dampen the tumor-inhibiting activity

(Zannikou *et al.*, 2023). IL-18, on the other hand, has been associated with systemic toxicities, including cytokine release syndrome (CRS) (Brandon *et al.*, 2024). In contrast, IL-23, a heterodimeric cytokine composed of two subunits (p19 and p40), has been shown to enhance the expansion and persistence of memory T-cells and Th17 cells, which are crucial for anti-cancer immunity of T-cells (Ma *et al.*, 2020). In this work, p40-H3BBz was designed to exploit the autocrine IL-23 signaling pathway. This autocrine signaling enhances the efficacy of H3BBz, as demonstrated by the elevated IL-23 and IFN-γ secretion in p40-H3BBz compared to H3BBz. This enhancement in tumor control mediated by p40-H3BBz was further supported by their superior tumor infiltration and persistence *in-vivo*. The toxicity, particularly on-target, off-tumor side effects of CAR T-cells, is a critical concern that warrants careful consideration. Importantly, evaluation of potential toxicity of p40-H3BBz was conducted and no significant tissue damage was observed, indicating that p40-H3BBz does not induce notable toxic side effects. Such findings are important for facilitating the translation of this therapeutic strategy.

CONCLUSION

The study demonstrates that targeting CD276 with p40-H3BBz shows stronger tumor-killing activity in NSCLC. The autocrine IL-23 signaling pathway is essential for enhancing the proliferation, survival and effector capacity of H3BBz within the TME. This study introduces a previously unreported approach to improving the anti-tumor potency of CAR T-cells to eradicate solid tumors and offers a new perspective for developing effective, targeted immunotherapies for NSCLC and potentially other solid tumors.

Acknowledgments
Not applicable.

Authors' contributions
Jianye Yang: Performed all experiments and analyzed the data; Ying Chen: Reviewed the data and wrote the manuscript. All authors read and approved the final version of the manuscript.

Funding
Medical and Health of Shaoxing (Grant no. 2023SKY087).

Data availability statement
The data supporting the findings of this study are available from the corresponding author upon reasonable request.

Ethical approval
All animal experiments were conducted in accordance with the guidelines approved by Shaoxing University (Approval number: 20236307). All experimental animals were accompanied by a quality certificate (SCXK 2023-0026). This study was performed in adherence with the ARRIVE guidelines. See supplementary file for the ARRIVE checklist.

Conflict of interest
The authors declare no conflicts of interest.

Supplementary data
https://www.pjps.pk/uploads/2026/05/SUP1779710717.pdf

REFERENCES

Allen GM, Frankel NW, Reddy NR, Bhargava HK, Yoshida MA, Stark SR, Purl M, Lee J, Yee JL, Yu W, Li AW, Garcia KC, El-Samad H, Roybal KT, Spitzer MH and Lim WA (2022). Synthetic cytokine circuits that drive T-cells into immune-excluded tumors. *Science,* **378**(6625): eaba1624.

Altan M, Pelekanou V, Schalper KA, Toki M, Gaule P, Syrigos K, Herbst RS and Rimm DL (2017). B7-H3 expression in NSCLC and its association with B7-H4, PD-L1 and tumor-infiltrating lymphocytes. *Clin Cancer Res,* **23**(17): 5202-09.

Boniface K, Blom B, Liu YJ and de Waal Malefyt R (2008). From interleukin-23 to T-helper 17 cells: human T-helper cell differentiation revisited. *Immunol Rev,* **226**: 132-46.

Brandon D Ng, Rajagopalan A, Kousa AI, Fischman JS, Chen S, Massa A, Elias HK, Manuele D, Galiano M, Lemarquis AL, Boardman AP, DeWolf S, Pierce J, Bogen B, James SE and van den Brink MRM (2024). IL-18-secreting multiantigen targeting CAR T-cells eliminate antigen-low myeloma in an immunocompetent mouse model. *Blood,* **144**(2): 171-86.

Cai D, Li J, Liu D, Hong S, Qiao Q, Sun Q, Li P, Lyu N, Sun T, Xie S, Guo L, Ni L, Jin L and Dong C (2020). Tumor-expressed B7-H3 mediates the inhibition of antitumor T-cell functions in ovarian cancer insensitive to PD-1 blockade therapy. *Cell Mol Immunol,* **17**(3): 227-36.

Chan JD, Scheffler CM, Munoz I, Sek K, Lee JN, Huang YK, Yap KM, Saw NYL, Li J, Chen AXY, Chan CW, Derrick EB, Todd KL, Tong J, Dunbar PA, Li J, Hoang TX, de Menezes MN, Petley EV, Kim JS, Nguyen D, Leung PSK, So J, Deguit C, Zhu J, House IG, Kats LM, Scott AM, Solomon BJ, Harrison SJ, Oliaro J, Parish IA, Quinn KM, Neeson PJ, Slaney CY, Lai J, Beavis PA and Darcy PK (2024). FOXO1 enhances CAR T-cell stemness, metabolic fitness and efficacy. *Nature,* **629**(8010): 201-10.

Chandrashekar DS, Karthikeyan SK, Korla PK, Patel H, Shovon AR, Athar M, Netto GJ, Qin ZS, Kumar S, Manne U, Creighton CJ and Varambally S (2022). UALCAN: An update to the integrated cancer data analysis platform. *Neoplasia,* **25**: 18-27.

Fan YP, Zhang YT, Zhang G, Ma L, Lv Y, Li J, Luan Y, Zhang YX, Chen YT, Ren HY, Liu W, Li MH, Wu YX, Chen S, Han B, Tang QY, Chen LH, Wesselius A, Su WC, Zeegers MP, Gu Y, Qin QR, Hao H, Xia J, Zhang H, Yu EY (2025). Proteomic profiling of urinary large extracellular vesicles for the diagnosis of prostate

cancer. *Anal Chem*, **97**(32):17368-79.

Feng S, Zhang Y, Wang Y, Gao Y, Song Y (2024). Harnessing gene editing technology for tumor microenvironment modulation: An emerging anticancer strategy. *Chemistry*, **30**(62): e202402485.

Getu AA, Tigabu A, Zhou M, Lu J, Fodstad O and Tan M (2023). New frontiers in immune checkpoint B7-H3 (CD276) research and drug development. *Mol Cancer,* **22**(1): 43.

Hong M, Clubb JD and Chen YY (2020). Engineering CAR-T-cells for next-generation cancer therapy. *Cancer Cell,* **38**(4): 473-88.

Hu G, Li G, Wen W, Ding W, Zhou Z, Zheng Y, Huang T, Ren J, Chen R, Zhu D, He R, Liang Y and Luo M (2022). Case report: B7-H3 CAR-T therapy partially controls tumor growth in a basal cell carcinoma patient. *Front Oncol,* **12**: 956593.

Li D, Wang R, Liang T, Ren H, Park C, Tai CH, Ni W, Zhou J, Mackay S, Edmondson E, Khan J, Croix BS and Ho M (2023). Camel nanobody-based B7-H3 CAR-T-cells show high efficacy against large solid tumours. *Nat Commun,* **14**(1): 5920.

Loo D, Alderson RF, Chen FZ, Huang L, Zhang W, Gorlatov S, Burke S, Ciccarone V, Li H, Yang Y, Son T, Chen Y, Easton AN, Li JC, Rillema JR, Licea M, Fieger C, Liang TW, Mather JP, Koenig S, Stewart SJ, Johnson S, Bonvini E and Moore PA (2012). Development of an Fc-enhanced anti-B7-H3 monoclonal antibody with potent antitumor activity. *Clin Cancer Res,* **18**(14): 3834-45.

Ma X, Shou P, Smith C, Chen Y, Du H, Sun C, Porterfield Kren N, Michaud D, Ahn S, Vincent B, Savoldo B, Pylayeva-Gupta Y, Zhang S, Dotti G and Xu Y (2020). Interleukin-23 engineering improves CAR T-cell function in solid tumors. *Nat Biotechnol,* **38**(4):448-59.

Parikh RH and Lonial S (2023). Chimeric antigen receptor T-cell therapy in multiple myeloma: A comprehensive review of current data and implications for clinical practice. *CA Cancer J Clin,* **73**(3): 275-85.

Pawlak M, DeTomaso D, Schnell A, Meyer Zu Horste G, Lee Y, Nyman J, Dionne D, Regan BML, Singh V, Delorey T, Schramm MA, Wang C, Wallrapp A, Burkett PR, Riesenfeld SJ anderson AC, Regev A, Xavier RJ, Yosef N and Kuchroo VK (2022). Induction of a colitogenic phenotype in Th1-like cells depends on interleukin-23 receptor signaling. *Immunity,* **55**(9): 1663-79 e6.

Qin L, Cheng X, Wang S, Gong G, Su H, Huang H, Chen T, Damdinjav D, Dorjsuren B, Li Z, Qiu Z, Bian J (2024). Discovery of novel aminobutanoic acid-based ASCT2 inhibitors for the treatment of non-small-cell lung cancer. *J Med Chem*, **67**(2): 988-1007.

Seaman S, Zhu Z, Saha S, Zhang XM, Yang MY, Hilton MB, Morris K, Szot C, Morris H, Swing DA, Tessarollo L, Smith SW, Degrado S, Borkin D, Jain N, Scheiermann J, Feng Y, Wang Y, Li J, Welsch D, DeCrescenzo G, Chaudhary A, Zudaire E, Klarmann KD, Keller JR, Dimitrov DS and St Croix B (2017). Eradication of tumors through simultaneous ablation of CD276/B7-H3-positive tumor cells and tumor vasculature. *Cancer Cell,* **31**(4): 501-15 e8.

Subhadarshani S, Yusuf N and Elmets CA (2021). IL-23 and the tumor microenvironment. *Adv Exp Med Biol,* **1290**:89-98.

Tang L, Shao H, Wu Y, Wang J, Qian X, He L, Huang H, Xu Z (2023). Dominant negative TGFbeta receptor II and truncated TIM3 enhance the antitumor efficacy of CAR-T-cell therapy in prostate cancer. *Int Immunopharmacol*, **124**(Pt A): 110807.

Vitanza NA, Wilson AL, Huang W, Seidel K, Brown C, Gustafson JA, Yokoyama JK, Johnson AJ, Baxter BA, Koning RW, Reid AN, Meechan M, Biery MC, Myers C, Rawlings-Rhea SD, Albert CM, Browd SR, Hauptman JS, Lee A, Ojemann JG, Berens ME, Dun MD, Foster JB, Crotty EE, Leary SES, Cole BL, Perez FA, Wright JN, Orentas RJ, Chour T, Newell EW, Whiteaker JR, Zhao L, Paulovich AG, Pinto N, Gust J, Gardner RA, Jensen MC and Park JR (2023). Intraventricular B7-H3 CAR T-cells for diffuse intrinsic pontine glioma: Preliminary first-in-human bioactivity and safety. *Cancer Discov,* **13**(1): 114-31.

Wang M, Herbst RS and Boshoff C (2021). Toward personalized treatment approaches for non-small-cell lung cancer. *Nat Med,* **27**(8): 1345-56.

Yang J, Zhou W, Li D, Niu T and Wang W (2023). BCMA-targeting chimeric antigen receptor T-cell therapy for multiple myeloma. *Cancer Lett,* **553**: 215949.

Yang M, Tang X, Zhang Z, Gu L, Wei H, Zhao S, Zhong K, Mu M, Huang C, Jiang C, Xu J, Guo G, Zhou L and Tong A (2020). Tandem CAR-T-cells targeting CD70 and B7-H3 exhibit potent preclinical activity against multiple solid tumors. *Theranostics,* **10**(17): 7622-34.

Zannikou M, Duffy JT, Levine RN, Seblani M, Liu Q, Presser A, Arrieta VA, Chen CJ, Sonabend AM, Horbinski CM, Lee-Chang C, Miska J, Lesniak MS, Gottschalk S and Balyasnikova IV (2023). IL15 modification enables CAR T-cells to act as a dual targeting agent against tumor cells and myeloid-derived suppressor cells in GBM. *J Immunother Cancer,* **11**(2).

Zhang ZY, Xu JH, Zhang JL, Lin YX and Ou-Yang J (2024). CD276 enhances sunitinib resistance in clear cell renal cell carcinoma by promoting DNA damage repair and activation of FAK-MAPK signaling pathway. *BMC Cancer,* **24**(1): 650.

Zhang J, Zhou ZZ, Chen K, Kim S, Cho IS, Varadkar T, Baker H, Cho JH, Zhou L and Liu XM (2023). A CD276-targeted antibody-drug conjugate to treat non-small lung cancer (NSCLC). *Cells,* **12**(19).

Zhang X, Guo H, Chen J, Xu C, Wang L, Ke Y, Gao Y, Zhang B and Zhu J (2023). Highly proliferative and hypodifferentiated CAR-T-cells targeting B7-H3 enhance antitumor activity against ovarian and triple-negative breast cancers. *Cancer Lett,* **572**: 216355.

doi.org/10.36721/PJPS.2026.39.8.221.1